Table IV. Concomitant Evolution of Internal Angles at Phosphorus, β and γ in Four Tetracyclic Tetraaminophosphoranes

	% along Berry coordinate	β,[a] deg	γ,[b] deg	ref
fluorocyclen-phosphorane	50	169.7[c]	145.2[c]	27
dicyclenphosphorane	32.9	169.6 ± 0.3	131.1 ± 0.3	28
bis(borane)cyclen-phosphorane	10.4	176.8 ± 0.9	125.6 ± 0.9	29
3	-15	183.3 ± 0.9	117.6 ± 0.9	this work

[a] Internal axial NPN angle at phosphorus (Figure 2). [b] Internal equatorial NPN angle at phosphorus (Figure 2). [c] No eds's were reported by the authors.

be estimated. If one nevertheless applies the dihedral angles method and unit bond lengths,[32] one finds that structure **3** is distorted by -15% along the Berry coordinate. This *negative* value means that this structure is not located between the idealized TP and SP structures but "before" the TP, i.e., that the N1-P-N3 angle closes "on the other side" with respect to the N2-P-N4 angle[33] (Figure 2). This small but significant tilt of the P-N3 bond toward the molybdenum atom may simply result from a better occupation of space after the equatorial P-Mo bond is bent down. The resulting relief in interactions between the apical/equatorial P-N bonds can also be seen in the smaller equatorial N2-P-N4 angle. The correlation between the increase in angle between the apical bonds and decrease in angle between the equatorial bonds when related molecules are compared (Table IV) is remarkable; compound **3** provides an extreme situation where the former is "larger" than 180° (183.3 ± 0.9°), and the latter is smaller than 120° (117.6 ± 0.9°).

The diastereoisomer that has formed comes as the enantiomeric pair in which the more space-demanding cyclopentadienyl ring lies on the side of a more flexible six-membered ring while the carbonyls lie atop a five-membered ring. The planar or close-to-planar geometry of the nitrogen atoms prevents satisfactory description of these five- and six-membered rings in terms of the usual chair or envelope conformations. The tetracyclic cyclam structure is distorted by the metal bridge, as shown by the difference between the angles formed by the mean planes of the fused cycles P, N4, C3, C4, C5, N1 and P, N1, C6, C7, N2 (97.6°), and by that of the fused cycles P, N3, C11, C12, N4 and P, N2, C8, C9, C10, N3 (120.5°).

Acknowledgment. We thank C. Onteniente for doing the artwork.

Registry No. 1a, 64317-99-3; **3**, 100016-82-8; **4**, 100016-83-9; **5**, 99829-54-6; **5'**, 99829-55-7; **6**, 99829-56-8; **7a**, 81121-01-9; **7b**, 99883-33-7; **7b'**, 99829-58-0; **8**, 99829-57-9; **9**, 81121-03-1; **10**, 81121-05-3; $Fe(NO)_2(CO)_2$, 13682-74-1; $CpMo(CO)_3Cl$, 12128-23-3; $CpW(CO)_3Cl$, 12128-24-4; $[Rh(CO)_2Cl]_2$, 14523-22-9.

Supplementary Material Available: Listings of observed and calculated structure factors, tables of atomic coordinates for hydrogen atoms, nonessential angles, and least-squares planes (17 pages). Ordering information is given on any current masthead page.

(32) Holmes, R. R.; Dieters, J. A. *J. Am. Chem. Soc.* **1977**, *99*, 3318.
(33) Holmes, R. R. in "Pentacoordinated Phosphorus"; American Chemical Society: Washington, D.C., 1980; Vol. 1.
(34) There are very few usable reflections beyond $\theta = 20°$, because of the inferior crystal quality and the use of Mo Kα radiation. This is not crucial, because there are a sufficient number of reflections left to carry out the refinement under good conditions; ten data were used to obtain each variable.
(35) The refinements were carried out with the weight $w = 1/\sigma^2$ for each reflection, and no corrections were made in the weights. The fact that the R factor is about twice the R_w factor is not unusual in such molecular crystals.
(36) In this paper the periodic group notation in parentheses is in accord with recent actions by IUPAC and ACS nomenclature committees. A and B notation is elimination because of wide confusion. Groups IA and IIA become groups 1 and 2. The d-transition elements comprise groups 3 through 12, and the p-block elements comprise groups 13 through 18. (Note that the former Roman number designation is preserved in the last digit of the new numbering: e.g., III → 3 and 13.)

Crystal Structure of Bis(trimethylammonium) Decabromotetracuprate(II): A Review of Stacking Patterns in Pseudoplanar $Cu_nX_{2n+2}^{2-}$ and $Cu_nX_{2n}L_2$ Oligomers

Urs Geiser,[1a] Roger D. Willett,*[1a] Martha Lindbeck,[1b] and Kenneth Emerson[1b]

Contribution from the Department of Chemistry, Washington State University, Pullman, Washington 99164-4630, and the Department of Chemistry, Montana State University, Bozeman, Montana 59715. *Received April 10, 1985*

Abstract: The stacking of planar, bibridged copper(II) halide oligomers is reviewed. Within each oligomer, the copper ions assume a nearly square-planar coordination. Interoligomer contacts lead to further semicoordination, yielding a 4 + 1 or 4 + 2 coordination for the copper ions. A wide variation in stacking patterns is observed, associated with many possible ways of forming the semicoordinate bonds. A simple graphic representation illustrating the stacking patterns is introduced, as well as a more detailed formal specification of the patterns. The crystal structure of a compound containing a new variant of these stacking patterns is also presented. $[(CH_3)_3NH]_2Cu_4Br_{10}$ is monoclinic, space group $P2_1/c$ with $a = 9.556$ (3) Å, $b = 14.703$ (4) Å, $c = 18.173$ (5) Å, $\beta = 99.75$ (3)°, $Z = 4$, and $\rho_{calcd} = 3.11$ g/cm^3. The structure, refined to an R value of 0.049, contains the nearly planar $Cu_4Br_{10}^{2-}$ oligomers,

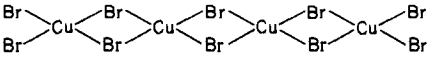

These stack such that three of the four copper ions have a 4 + 2 coordination geometry, while the fourth has only a 4 + 1 coordination geometry.

I. Introduction

The crystal chemistry of copper(II) halides is extremely diverse and complex. This is certainly due, at least in part, to the presence of an active Jahn-Teller effect in these d^9 electronic systems. Thus, true octahedral complexes are not known; rather distortions of the nominally six-coordinate complexes occur, leading, generally, to an elongation of the copper-ligand (Cu-L) bond lengths along one axis. This gives a typical 4 + 2 coordination geometry with

(1) (a) Washington State University. (b) Montana State University.

0002-7863/86/1508-1173$01.50/0

four short Cu–L bonds and two longer, or semicoordinate, Cu–L interactions. We have used the criterion that a ligand, L′, is semicoordinate when the L–L′ distance is greater than the sum of the ligand van der Waal radii.[2] This is the case, for example, in the layer perovskites of the type $(RNH_3)_2CuX_4$.[3] Another factor in the complexity of the coordination geometry in copper(II) halide systems is the relative flatness of the potential surfaces for many distortions.[4] Thus, in tetracoordinate CuX_4^{2-} salts, a continuum of geometries exists from square planar to nearly tetrahedral.[5] This appears to be due to a counteraction of crystal-field stabilization effects and ligand–ligand electrostatic repulsions. This has lead us to postulate the concept of charge compensation to explain many of the features observed in copper(II) halide crystal systems.[2] Thus, in CuX_4^{2-} systems, when hydrogen bonding or other electrostatic interactions remove charge from the ligands, the geometry tends toward planarity, while an "isolated" ion will have a geometry close to tetrahedral. The situation can also be confused by dynamical effects, as exemplified by the $CuCl_5^{3-}$ ion found in $Cr(NH_3)_6CuCl_5$ and $Co(NH_3)_6CuCl_5$.[6] Orginally cited as a true trigonal-bipyramidal five-coordinate species, recent studies have shown that the room-temperature structure is actually a dynamical superposition of three square-pyramidal species.[7]

We have recently been interested in the structures of $ACuCl_3$ salts.[8] Three general structure types were described: $Cu_2Cl_6^{2-}$ dimers existing as isolated ions or aggregated in stacks; symmetrically bibridged chains with square-pyramidal coordination geometry; and tribridged chains based on Jahn–Teller distortions of the $CsNiCl_3$ structure. For the aggregated stacks of dimers, we introduced a simple graphical representation for the diffeent types of stacking patterns observed in these systems. The interest in the structural properties of these $ACuX_3$ systems lead us to follow up on the report of the compound $(CH_3)_3NHCuBr_3$.[9] Attempted syntheses of this salt yielded instead the compound $[(CH_3)_3NH]_2Cu_4Br_{10}$. This paper presents a general review and discussion of the crystal chemistry of $Cu_nX_{2n+2}^{2-}$ and $Cu_nX_{2n}L_2$ oligomers followed by the results of the structural investigation of $[(CH_3)_3NH]_2Cu_4Br_{10}$.

II. Stacking Patterns

A. General. The discussion of the stacking in these $Cu_nX_{2n+2}^{2-}$ and $Cu_nX_{2n}L_2$ oligomers begins with the cubic close-packed structures of the MX_2 types such as exhibited by CdI_2. In these salts, half of the octahedral holes are occupied by the divalent metal ions to form hexagonal layers of edge-shared octahedra. When Cu(II) is placed on this lattice, the Jahn–Teller effect operative in these d^9 ions causes a distortion of the lattice. The distortion is ferroelastic; that is, the axes of elongation are parallel for all octahedra. In this manner, clearly identifiable bibridged chains are defined in $CuCl_2$, for example, with short (2.3 Å) Cu–Cl bonds within the chains and longer (~3.0 Å) Cu–Cl bonds between the chains.[10]

It is possible to interrupt these infinite chains either with coordinating ligands or with counterions, forming planar, bibridged oligomers with the general formula $Cu_nX_{2n}L_2$ or $Cu_nX_{2n+2}^{2-}$. In the compounds known so far, n ranges formally from 1 (e.g., $CuCl_2 \cdot 2H_2O$ or the $CuCl_4^{2-}$ ion) to 5 for $Cu_5Cl_{10}(C_3H_7OH)_2$. The additional ligands (L or X^-), together with the spatial and H-bonding requirements of the counterion in the ionic compounds,

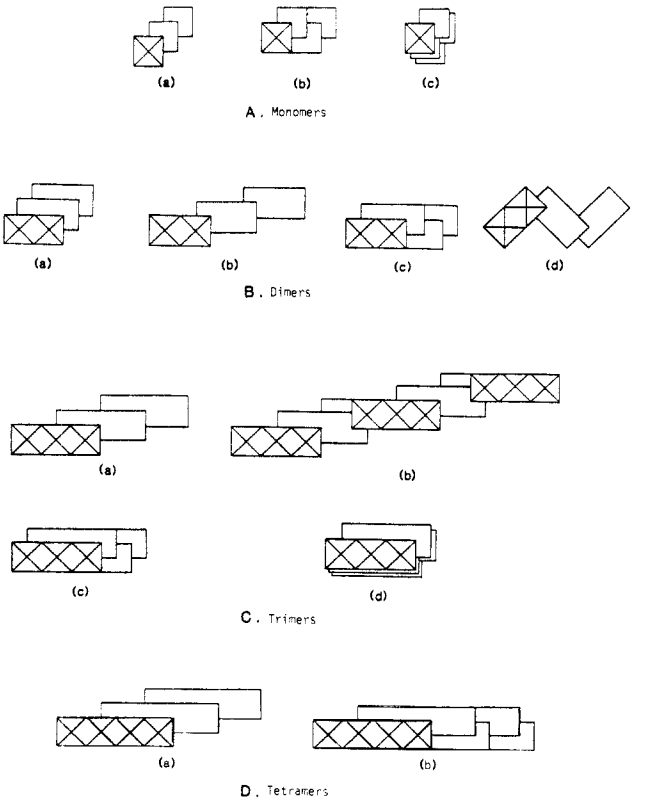

Figure 1. Stacking patterns for pseudoplanar $Cu_nX_{2n}L_2$ oligomers.

may interrupt the chains in different manners, often forcing rearrangement of the relative position of adjacent oligomers and yielding a variety of different stacking patterns. These are illustrated in Figure 1 for the various structures observed to date. It is the variations in these patterns which we wish to focus upon. Since there exists a complex variety of patterns, we wish to introduce a notation to specify them. Of necessity, this notation will be somewhat complex, but we hope it will provide a unique description of the principal patterns.

B. Nomenclature. The notation introduced to describe the possible stacking patterns of $Cu_nX_{2n+2}^{2-}$ or $Cu_nX_{2n}L_2$ oligomers in crystalline solids specifies the displacement of the oligomer of n Cu atoms in terms of the ligand–ligand distances, d, along its edges. It is necessary to specify two displacements—one translation of length $m_{\parallel}d$ parallel to the Cu–Cu direction and a second translation of length $m_{\perp}d$ perpendicular to the Cu–Cu direction. (For monomers, the displacements are along two orthogonal axes bisecting cis L–Cu–L bond directions.) This yields a symbol $(m_{\parallel},m_{\perp})$ to specify the displacement of adjacent oligomers. As many symbols are concatenated as are necessary to create the basic repeat unit along the stack. Thus, a notation $n(m_{\parallel},m_{\perp})$ would indicate an oligomer of length n with a single type of displacement specifying the repeat unit, while the notation $n(m_{\parallel},m_{\perp})(m_{\parallel}',m_{\perp}')$ would indicate that the repeat unit consists of alternating displacements $(m_{\parallel},m_{\perp})$ and $(m_{\parallel}',m_{\perp}')$.

In some cases, it is also necessary to add a specification of a rotation about the normal to the plane of the oligomer in addition to the translation operations. This we may do by adding (when necessary) a third, rotational component to the vector, yielding a notation $(m_{\parallel},m_{\perp},\phi)$. The rotation is about the Cu(undisplaced oligomer)–Cl(displaced oligomer) bond thus formed. Again, a repetition of the vector will be used to specify alternating directions of rotation.

It is to be noted that any single vector pattern is simply derived from the basic CuX_2 structure by appropriately cutting a slice from the stacks in that structure. On the other hand, the multiple vector patterns will involve often a rearrangement of the basic CuX_2 stacking pattern.

With each pattern, we have also introduced a simple graphical representation of the stacking (Figure 1). This supplements the

(2) Willett, R. D. In "Magneto-Structural Correlations in Exchanged Coupled Systems"; Willett, R. D., Gatteschi, D., Kahn, O., Eds.; D. Reidel Publishing Co.: New York, 1985; NATO Advanced Study Institute Series.
(3) Willett, R. D.; Jardine, F. H.; Rouse, I.; Wong, R. J.; Landee, C. P.; Numata, M. *Phys. Rev.* **1981**, *B24*, 5372 and references therein.
(4) Lohr, L. L.; Lipscomb, W. N. *Inorg. Chem.* **1963**, *2*, 911.
(5) Willett, R. D.; Haugen, J. A.; Lebsack, J.; Morrey, J. *Inorg. Chem.* **1974**, *13*, 2510.
(6) Bernal, I.; Korp, J. D.; Schlemper, E. O.; Hussain, M. S. *Polyhedron* **1982**, *1*, 365.
(7) Reinen, D.; Friebel, C. *Inorg. Chem.* **1984**, *23*, 791.
(8) Willett, R. D.; Geiser, U. *Croat. Chem. Acta* **1984**, *57*, 737.
(9) Amiel, J. *C. R. Hebd. Seances Acad. Sci.* **1937**, *205*, 1400.
(10) Wells, A. F. *J. Chem. Soc.* **1947**, 1670.

Table I. Stacking Patterns of $Cu_nX_{2n+2}^{2-}$ and $Cu_nX_{2n}L_2$ Oligomers

symbol	oligomer	compound	ref
	Monomers		
$1(^1/_2,^1/_2)$	$CuCl_2(H_2O)_2$	$CuCl_2(H_2O)_2$	14
	$CuCl_2(py)_2$	$CuCl_2(py)_2$	15a
$1(^1/_2,^1/_2)(^1/_2,^{-1}/_2)$	$CuCl_2(oxime)_2$	$Cu(C_{14}H_{12}N_2O_2)Cl_2$	16
$1(^1/_2,^1/_2)(^{-1}/_2,^{-1}/_2)$	$CuCl_3(N_2H_5)$	$N_2H_5CuCl_3$	17a
	$CuCl_2(C_2H_6N_4O_2)$	$CuCl_2(C_2H_6N_2O_2)$	17b
	Dimers		
$2(^1/_2,^1/_2)$	$Cu_2Cl_6^{2-}$	$KCuCl_3$	11
		NH_4CuCl_3	11, 19
	$Cu_2Br_6^{2-}$	$KCuBr_3$	18
	$Cu_2Cl_4(CH_3CN)_2$	$Cu_2Cl_4(CH_3CN)_2$	20
	$Cu_2Br_4(py)_2$	$Cu_2Br_4(py)_2$	21
$2(^3/_2,^1/_2)$	$Cu_2Cl_6^{2-}$	$LiCuCl_3{\cdot}2H_2O$	22
		$(CH_3)_2CHNH_3CuCl_3$	23
		$(C_5N_4H_5)Cu_2Cl_6$	28
		$(C_4N_2H_{12})Cu_2Cl_6$	25
		$(C_{12}H_{14}N_2)Cu_2Cl_6$	26
		$[(C_6H_5)CH_2CH_2NH_2(CH_3)]CuCl_3$	27
	$Cu_2Br_6^{2-}$	$(CH_3)_2CHNH_2CuBr_3$	24
	$Cu_2Cl_4(pyNO)_2$	$Cu_2Cl_4(pyNO)_2$	29
	$Cu_2Cl_2(OCH_3)_2py_2$	$Cu_2Cl_2(OCH_3)_2py_2$	30
$2(^1/_2,^1/_2)(^1/_2,^{-1}/_2)$	$Cu_2Cl_6^{2-}$	$(C_3N_6H_8)Cu_2Cl_6$	25, 31
$2(^3/_2,^1/_2,90°)(^3/_2,^{-1}/_2,-90°)$	$Cu_2Cl_6^{2-}$	$(CH_3)_2NH_2CuCl_3$	13
		$(C_6H_5)CH_2C_5NH_{11}CuCl_3$	32
		$(C_5NH_{12})CuCl_3$	25
	Trimers		
$3(^3/_2,^1/_2)$	$Cu_3Cl_6(CH_3CN)_2$	$Cu_3Cl_6(CH_3CN)_2$	20
	$Cu_3Cl_6(H_2O)_2$	$Cu_3Cl_6(H_2O)_2(C_4H_8SO_2)_2$	33
$3(^1/_2,^1/_2)(^{-1}/_2,^1/_2)$	$Cu_3Cl_8^{2-}$	$(CH_3C_4N_2H_{11})_2Cu_3Cl_8$	25
$3(^1/_2,^1/_2)(^{-1}/_2,^{-1}/_2)$	$Cu_3Br_8^{2-}$	$[(C_2H_5)_2NH_2]_2Cu_4Br_{10}{\cdot}2EtOH$	12
	Tetramers		
$4(^3/_2,^1/_2)$	$Cu_4Cl_{10}^{2-}$	$[(CH_3)_3NH]_2Cu_4Cl_{10}$	34
$4(^3/_2,^1/_2)(^1/_2,^{-1}/_2)$	$Cu_4Br_{10}^{2-}$	$[(CH_3)_3NH]_2Cu_4Br_{10}$	this work
	Pentamers		
$5(^3/_2,^1/_2)$	$Cu_5Cl_{10}(C_3H_7OH)_2$	$Cu_5Cl_{10}(C_3H_7OH)_2$	20

notation introduced and, since a picture is worth a thousand words, lends clarity to the discussion of the stacking patterns.

In the following sections, we illustrate this notation by utilizing several representative oligomers.

C. Examples. 1. $Cu_2Cl_6^{2-}$ Stacks in $KCuCl_3$.[11] As illustrated in Figure 1B(a), the stacking consists of displacing each successive dimer such that one of the terminal chloride ions is directly below the corresponding copper(II) ion in the previous dimer. That is, the displacement is specified by $(^1/_2,^1/_2)$, and since each successive displacement is identical, the notation for the stack is $2(^1/_2,^1/_2)$.

This is one of the simplest examples of oligomer stacking derived from the parent CuX_2 structure. The planar dimers stack in exactly the same manner as the chains in anhydrous $CuCl_2$ with adjacent dimers related by unit cell translations of approximately 4.0 Å. This translation gives a distorted 4 + 2 coordination geometry for each copper(II) ion as in $CuCl_2$. In this manner, four long Cu–Cl bonds are formed between each pair of dimers.

2. $Cu_3Br_8^{2-}$ Ions in $[(C_2H_5)_2NH_2]_2Cu_4Br_{10}{\cdot}EtOH$.[12] In this structure, the trimers lie on mirror planes and adjacent trimers are related by a 2-fold screw axis parallel to the normal to the plane and intersecting one of the Cu–Br bonds of the central copper(II) ion. This is illustrated in Figure 1C(b) and is specified by the notation $3(^1/_2,^1/_2)(^{-1}/_2,^{-1}/_2)$. Thus, the stacking is very different than in the parent CuX_2. Succeeding displacements alternate directions so that the unit cell translation along the stacking direction is normal to the plane of the trimers. The repeat distance is about 6.4 Å and involves two displacements. Again, this leads to a 4 + 2 coordination for each copper ion in the trimer, with a total of six long Cu–Br bonds between adjacent trimers.

Table II. Experimental Data for the X-ray Diffraction Study of Crystalline $[(CH_3)_3NH]_2Cu_4Br_{10}$

temperature: 25 °C
crystal habit and dimensions: flat needle, 0.6 mm × 0.1 mm × 0.06 mm
crystal system: monoclinic
space group: $P2_1/c$
cell parameters
  a = 9.556 (5) Å
  b = 14.703 (4) Å
  c = 18.173 (5) Å
  β = 99.75 (3)°
  V = 2516 (2) Å^3
  z = 4
  ρ_c = 3.11 g/cm^3
data collection parameters:
  diffractometer: Nicolet R3m/E
  radiation: MoKα (λ = 0.71069 Å)
  monochromator: graphite crystal
  refl. collected: $+h,+k,\pm l$
  2θ range: 3.0–40.0°
  scan type: Wyckoff ω scans
  scan speeds: 4–29.3°/min
  std. refl: 3 collected every 100 refl; no significant changes in intensity observed
  reflections collected: 2752
  reflections observed: 1627 ($5\sigma_1$ cutoff)
  abs coeff: 160 cm^{-1}; empirical absorption corrections fitted to a set of eight ψ scans
  programs used: SHELXTL system of R3m/E

3. $Cu_2Cl_6^{2-}$ Ions in $(CH_3)_2NH_2CuCl_3$.[13] In this case, the stacking involves a rotation as well as a displacement such that the stacking pattern of the parent CuX_2 lattice is completely

(11) Willett, R. D.; Dwiggins, C., Jr.; Kruh, R. F.; Rundle, R. E. *J. Chem. Phys.* **1963**, *38*, 2429.
(12) Fletcher, R.; Hansen, J. J.; Livermore, J.; Willett, R. D. *Inorg. Chem.* **1982**, *22*, 330.
(13) Willett, R. D. *J. Chem. Phys.* **1966**, *44*, 39.

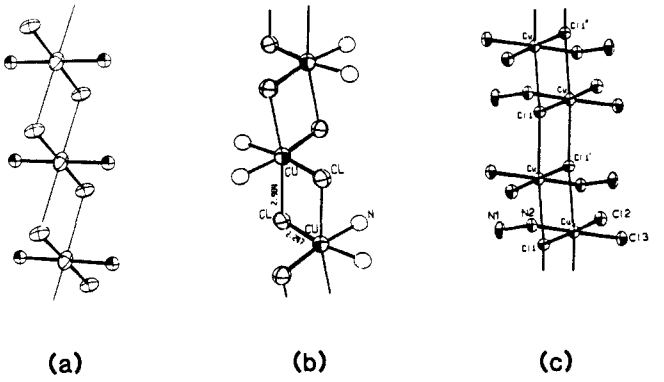

Figure 2. Stacking of CuX_2L_2 monomers. (a) Uniform chain in $CuCl_2(4\text{-Mepy})_2$. (b) Ladder chain in $(N_2H_5)CuCl_3$. (c) Zig-zag chain in $Cu(C_{14}H_{12}N_2O_2)Cl_2$.

broken. The pattern is represented by the symbol $2(^3/_2, ^1/_2, 90°)(^3/_2, -^1/_2, -90°)$ and is illustrated schematically in Figure 1B(b). The dimer is displaced in such a manner that one copper is moved to a position below a terminal chlorine on the opposite end of the dimer and then rotated approximately 90° about that Cu–Cl axis. In the next displacement, the rotation is in the opposite sense. This creates a zig-zag chain, with unit cell translation (between alternate dimers) of approximately 12 Å. It yields a 4 + 1 coordination for each copper(II) ion.

D. Summary of Known Structures. 1. $n = 1$ (Monomers). (a) $1(^1/_2, ^1/_2)$ Patterns (Figure 1A(a)). These are exhibited by salts such as $CuCl_2 \cdot 2H_2O$,[14] $CuCl_2 \cdot 2py$,[15a] and related compounds, and the stacking pattern is illustrated in Figure 2a for $CuCl_2(4\text{-methylpyridine})_2$.[15b] The stacking yields a repeat distance of approximately 4.0 Å and gives a 4 + 2 coordination for each copper ion.

(b) $1(^1/_2, ^1/_2)(-^1/_2, ^1/_2)$ Patterns (Figure 1A(b)). These are the so-called zig-zag chains such as recently reported in $Cu(C_{14}H_{12}N_2O_2)Cl_2$.[16] The stacking pattern (Figure 2b) again yields a 4 + 2 coordination geometry but with a repeat distance of 6.9 Å.

(c) $1(^1/_2, ^1/_2)(-^1/_2, -^1/_2)$ Patterns (Figure 1A(c)). This is observed in $(N_2H_5)CuCl_3$,[17a] Figure 2c, and yields a 4 + 2 coordination geometry with a repeat distance of 5.7 Å, approximately twice the axial Cu–Cl distance. The same stacking pattern, but with longer axial Cu–Cl bonds (3.14 Å) is found in the oxamide dioxime complex, $CuCl_2(C_2H_6N_4O_2)$.[17b]

It should be noted that this nomenclature cannot be used to describe the packing of $CuCl_4^{2-}$ monomers in the two-dimensional layer structures assumed by $(RNH_3)_2CuX_4$ salts.

2. $n = 2$ (Dimers). (a) $2(^1/_2, ^1/_2)$ Patterns (Figure 1B(a)). These include $KCuCl_3$,[11] NH_4CuCl_3,[11,19] $KCuBr_3$,[18] $Cu_2Cl_4(CH_3CN)_2$,[20] and $Cu_2Br_4(py)_2$.[21] The basic structure description was given in the previous section, and an ORTEP drawing is given in Figure 3a.

(b) $2(^3/_2, ^1/_2)$ Patterns (Figure 1B(b)). These include $LiCuCl_3 \cdot 2H_2O$,[22] the low-temperature forms of $(CH_3)_2CHNH_3CuCl_3$,[23] and $(CH_3)_2CHNH_3CuBr_3$,[24] (piperazinium)Cu_2Cl_6,[25] (paraquat)Cu_2Cl_6,[26] $[(C_6H_5)CH_2CH_2NH_2(CH_3)]CuCl_3$,[27] as well as (purinium)Cu_2Cl_6.[28] As is the case in the $2(^1/_2, ^1/_2)$ patterns, this stacking is simply derived from the basic CuX_2 stacks, except that the first copper(II) ion in each dimer is displaced to a position beneath one of the terminal chlorides, rather than to a bridging chloride. As seen in Figure 3b for $(CH_3)_2CHNH_3CuBr_3$, this type of displacement allows for more distortion of the oligomers from planarity, especially involving the terminal halide ions. It leads to a 4 + 1 coordination geometry for each copper(II) ion in the idealized structure. However, the sixth octahedral position can be occupied by additional ligands. Thus, in $LiCuCl_3 \cdot 2H_2O$, each copper expands to a 4 + 2 coordination by bonding to a water molecule. In the purinium salt, on the other hand, one of the copper ions retains its 4 + 1 geometry, while one of the unprotonated nitrogen atom in the purinium ions bonds to the other copper ion, expanding its coordination to 4 + 2. Also included in this category are the oxygen bridged dimers with pyridine *N*-oxide, $Cu_2Cl_4(pyNO)_2$,[29] the methoxide ion, $Cu_2Cl_2(OCH_3)_2py_2$,[30a] and other more complex alkoxide bridged species.[30b]

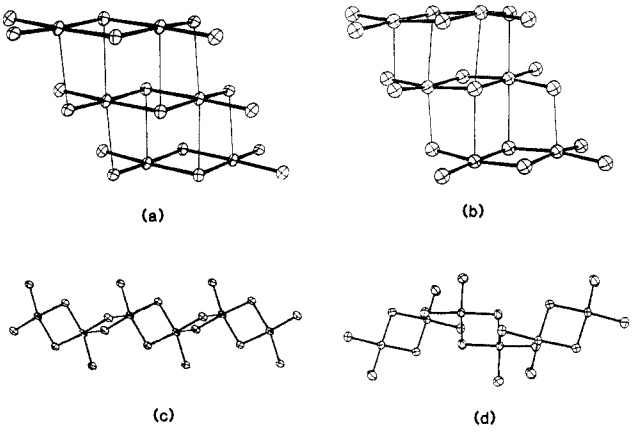

Figure 3. Stacking of $Cu_2X_4L_2$ oligomers. (a) $Cu_2Cl_6^{2-}$ dimers in $KCuCl_3$. (b) $Cu_2Cl_6^{2-}$ dimers in $(CH_3)_2NH_2CuBr_3$. (c) $Cu_2Cl_6^{2-}$ dimers in (melamineH_2)Cu_2Cl_6. (d) $Cu_2Cl_6^{2-}$ dimers in $(CH_3)_2CHNH_3CuCl_3$.

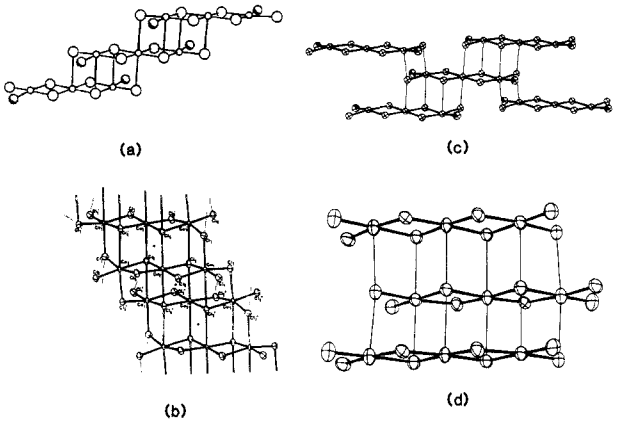

Figure 4. Stacking of $Cu_3X_6L_2$ oligomers. (a) Stacking of $Cu_3Cl_6(H_2O)_2$ trimers in $Cu_3Cl_6(H_2O)_2(C_4H_8SO_2)_2$. (b) Stacking of $Cu_3Cl_8^{2-}$ trimers in $(CH_3C_4N_2H_{11})CuCl_3$. (c) Stacking of $Cu_3Cl_6(CH_3CN)_2$ trimers. (d) Stacking of $Cu_3Br_8^{2-}$ trimer in $[(C_2H_5)_2NH_2]_2Cu_4Br_{10} \cdot EtOH$.

(14) Harker, D. *Z. Kristallogr.* **1936**, *93*, 136.
(15) (a) Morosin, B. *Acta Crystallogr., Sect. B* **1975**, *B31*, 632. (b) Marsh, W. E.; Valente, E. J.; Hodgson, D. J. *Inorg. Chim. Acta* **1981**, *51*, 49.
(16) Mégnamisi-Bélombé, M.; Singh, P.; Bolster, D. E.; Hatfield, W. E. *Inorg. Chem.* **1984**, *23*, 2578.
(17) (a) Brown, D. B.; Donner, J. A.; Hall, J. W.; Wilson, S. R.; Wilson, R. B.; Hodgson, D. J.; Hatfield, W. E. *Inorg. Chem.* **1979**, *18*, 2635. (b) Endres, H. *Acta Crystallogr., Sect. C* **1983**, *C39*, 1192.
(18) Dwiggins, C., Jr. Ph.D. Thesis, University of Arkansas, 1960.
(19) O'Bannon, G.; Willett, R. D. *Inorg. Chim. Acta* **1981**, *53*, L131.
(20) Willett, R. D.; Rundle, R. E. *J. Chem. Phys.* **1964**, *40*, 838.
(21) Swank, D. D.; Willett, R. D. *Inorg. Chem.* **1980**, *19*, 2321.
(22) Vossos, P. H.; Fitzwater, D. R.; Rundle, R. E. *Acta Crystallogr.* **1963**, *16*, 1037.
(23) Roberts, S. A.; Bloomquist, D. R.; Willett, R. D.; Dodgen, H. W. *J. Am. Chem. Soc.* **1981**, *103*, 2603.
(24) Bloomquist, D. R.; Willett, R. D. *J. Am. Chem. Soc.* **1981**, *103*, 2615.
(25) Manfredini, T. Ph.D. Thesis, Universities of Modena and Bologna, Italy, 1984.
(26) Murray-Rust, P. *Acta Crystallogr., Sect B* **1975**, *B31*, 1771.
(27) Harlow, R. L.; Wells, W. J., III; Watt, G. W.; Simonsen, S. H. *Inorg. Chem.* **1974**, *13*, 2860.
(28) Sheldrick, W. S. *Acta Crystallogr., Sect. B* **1981**, *B37*, 945.
(29) Sager, R. S.; Williams, R. J.; Watson, W. H. *Inorg. Chem.* **1967**, *6*, 951; *Inorg. Chem.* **1969**, *8*, 694.
(30) (a) Willett, R. D.; Breneman, G. L. *Inorg. Chem.* **1983**, *22*, 326. (b) Walz, L.; Paulus, H.; Haase, W. *J. Chem. Soc., Dalton Trans.* **1985**, 913 and references therein.

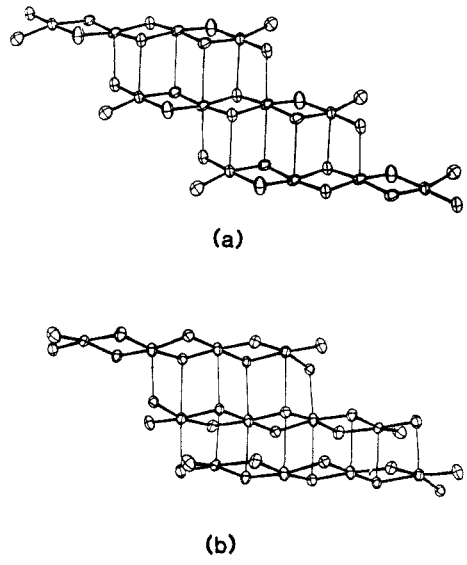

Figure 5. Stacking of $Cu_4X_8L_2$ oligomers. (a) $Cu_4Cl_{10}^{2-}$ tetramers in $(TMA)_2Cu_4Cl_{10}$. (b) $Cu_4Br_{10}^{2-}$ tetramers in $(TMA)_2Cu_4Br_{10}$.

(c) $2(^1/_2,^1/_2)(^1/_2,-^1/_2)$ Patterns (Figure 1B(c)). This is exhibited by (melaminium)Cu_2Cl_6[31] and involves an alternation of the displacement perpendicular to the Cu–Cu direction. Thus, the projection of the repeat translation along the stack onto the dimer is parallel to the Cu–Cu direction. This yields essentially a 4 + 2 coordination geometry for each Cu atom, although the two long Cu–Cl distances are quite different from each other. An illustration is given in Figure 3c.

(d) $2(^3/_2,^1/_2,$90°$)(^3/_2,-^1/_2,-$90°$)$ Patterns (Figure 1b(d)). This is assumed by $(CH_3)_2NH_2CuCl_3$,[13] (4-benzylpiperidinium)$CuCl_3$,[32] and (piperidinium)$CuCl_3$[25] and was described in the previous section. An ORTEP drawing of the dimethylammonium salt is given in Figure 3d.

3. n = 3 (Trimers) (Figure 8). (a) $3(^3/_2,^1/_2)$ Patterns (Figure 1C(a)). This type occurs in $Cu_3Cl_6(H_2O)_2{\cdot}2TMSO_2$,[33] and in $Cu_3Cl_6(CH_3CN)_2$,[20] and is essentially the same as the analogous dimer pattern with a 6.1-Å repeat distance along the stack. By itself, it would yield a 4 + 1 coordination for the two end copper(II) ions and a 4 + 2 coordination for the central copper(II) ion. In both structures, however, the end ions expand their coordination to 4 + 2: in the $TMSO_2$ complex by coordination to an oxygen of the sulfone group (Figure 4a); in the acetonitrile complex by interaction with adjacent stacks (Figures 1C(b) and 4b). This latter interaction yields an alternative stacking pattern of the type $3(-^5/_2,^1/_2)$.

(b) $3(^1/_2,^1/_2)(-^1/_2,-^1/_2)$ Patterns (Figure 1C(c)). This pattern, illustrated in Figure 4c, is found in $[(C_2H_5)_2NH_2]_2Cu_4Br_{10}{\cdot}C_2H_5OH$[12] and was described previously.

(c) $3(^1/_2,^1/_2)(^1/_2,-^1/_2)$ Patterns (Figure 1C(d)). This is found in (*N*-methylpiperazinium)Cu_3Cl_8[25] and again is basically the same as the corresponding $2(^1/_2,^1/_2)(^1/_2,-^1/_2)$ structure. A 4 + 2 coordination is assumed by each copper(II) ion, but the intertrimer Cu–Cl distances to the terminal chloride ions are much shorter than those to the bridging chloride ions (Figure 4d).

4. n = 4 (Tetramers). (a) $4(^3/_2,^1/_2)$ Patterns (Figure 1D(a)). This is found in $[(CH_3)_3NH]_2Cu_4Cl_{10}$[34] and yields a structure in which the two end copper(II) ions have a 4 + 1 coordination geometry while the two central copper(II) ions have a 4 + 2 configuration, as illustrated in Figure 5a.

(b) $4(^3/_2,^1/_2)(^1/_2,-^1/_2)$ Patterns (Figure 1D(4)). This is the pattern found in the structure reported in the following section of this paper and is illustrated in Figure 5b.

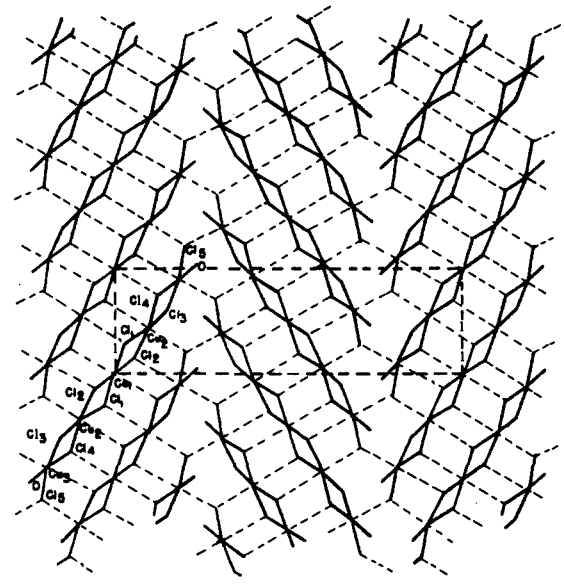

Figure 6. Stacking of pentamers in $Cu_5Cl_{10}(C_3H_7OH)_2$.

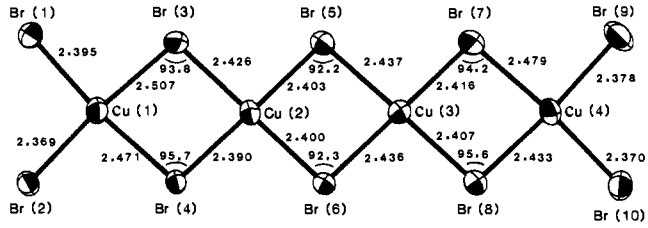

Figure 7. $Cu_4Br_{10}^{2-}$ ion in $(TMA)_2Cu_4Br_{10}$.

5. n = 5 (Pentamers). $5(^3/_2,^1/_2)$ Patterns. The $Cu_5Cl_{10}(C_3H_2OH)_2$ pentamer[20] assumes this pattern. By itself, the two end copper(II) ions would have a 4 + 1 coordination. However, as seen in Figure 6, they expand their coordination to 4 + 2 by bridging to chlorides in adjacent stacks.

III. Structure of $[(CH_3)_3NH]_2Cu_4Br_{10}$

Experimental. In order to prepare samples of $(CH_3)_3NHCuBr_3$, solutions of different proportions of $(CH_3)_3NHBr$ and $CuBr_2$ in dilute HBr solution were prepared and allowed to evaporate. Solutions with a ratio of 1:1.5 yielded dark violet, essentially opaque, needles. Chemical analysis indicated that the correct stoichiometry for the compound was $(CH_3)_3NHCu_2Br_5$. [Anal. Calcd: Cu, 21.66; Br, 68.10. Found: Cu, 20.03; Br, 65.98.] The compound was found to be monoclinic, $P2_1/c$ (systematic absences: $k = 2n + 1$ for $0k0$, $l = 2n + 1$ for $h0l$) with the needle axis parallel to a. Lattice constants, determined from the accurate centering of 20 high-angle reflections are a = 9.556 (5) Å, b = 14.703 (4) Å, c = 18.173 (5) Å, and β = 99.75 (3)°. Crystallographic data are listed in Table II.

The structure was solved from a Patterson map based on a data set collected at Washington State University. The data set was seriously affected by crystal decomposition and excessive absorption. Independently, the compound was synthesized and a data set collected at Montana State University. In that drier climate there was no evidence of decomposition in the course of the data collection. The solution found at WSU was used as a trial structure for least-squares refinement; copper and bromine atoms were refined with anisotropic temperature factors in the final refinements, whereas the carbon and nitrogen thermal parameters were retained isotropic. Final values of residuals were R = 0.0492 and R_w = 0.0501 ($R = \sum||F_o| - |F_c||/\sum|F_o|$; $R_w = [\sum w(|F_o| - |F_c|)^2/\sum w|F_o|^2]^{1/2}$. A final difference map had numerous peaks with heights of about 0.9 e/Å^3, clustered around the copper and bromine positions. Hydrogen atoms were searched for but not found. Positional parameters are listed in Table III, and the thermal parameters for the non-hydrogen atoms are given in Table IV. Important interatomic distances and angles are given

(31) Colombo, A.; Menabue, L.; Motori, A.; Pellacani, G. C.; Porzio, W.; Sandrolini, I.; Willett, R. D. *Inorg. Chem.* **1985**, *24*, 2900.
(32) Battaglia, L. P.; Bonamartini-Corradi, A.; Marcotrigiano, G.; Menabue, L.; Pellacani, G. C. *Inorg. Chem.* **1980**, *19*, 125.
(33) Swank, D. D.; Willett, R. D. *Inorg. Chim. Acta* **1974**, *8*, 143.
(34) Caputo, R. E., Vukosavovich, M. J.; Willett, R. D. *Acta Crystallogr., Sect. B* **1976**, *B32*, 2516.

Table III. Atomic Coordinates ($\times 10^4$) and Isotropic Thermal Parameters ($Å^2 \times 10^3$)

	x	y	z	U[a]
Cu(1)	-447 (4)	3406 (3)	6211 (2)	40 (2)*
Cu(2)	2114 (4)	4894 (3)	5588 (2)	38 (2)*
Cu(3)	4413 (4)	6444 (3)	4963 (2)	35 (2)*
Cu(4)	7194 (4)	7810 (3)	4439 (2)	36 (2)*
Br(1)	-2092 (4)	2341 (2)	5546 (2)	38 (1)*
Br(2)	-1434 (4)	3379 (3)	7321 (2)	48 (2)*
Br(3)	548 (4)	3684 (2)	5040 (2)	34 (1)*
Br(4)	1053 (4)	4720 (2)	6680 (2)	37 (1)*
Br(5)	3039 (4)	5125 (2)	4453 (2)	35 (1)*
Br(6)	3641 (4)	6094 (2)	6142 (2)	39 (1)*
Br(7)	5526 (4)	6613 (3)	3873 (2)	41 (1)*
Br(8)	6046 (4)	7595 (3)	5523 (2)	47 (2)*
Br(9)	8134 (4)	7938 (3)	3313 (2)	49 (2)*
Br(10)	8275 (4)	9167 (3)	4961 (2)	61 (2)*
N(1)	8610 (35)	11187 (22)	3756 (18)	74 (11)
C(11)	9111 (37)	12157 (25)	3656 (21)	54 (11)
C(12)	9140 (42)	10487 (30)	3268 (23)	76 (14)
C(13)	7024 (43)	11164 (26)	3654 (21)	65 (12)
N(2)	-3038 (30)	1214 (19)	6987 (16)	57 (9)
C(21)	-3839 (46)	1516 (31)	7608 (24)	87 (15)
C(22)	-1625 (43)	854 (29)	7256 (22)	75 (13)
C(23)	-3965 (45)	649 (31)	6462 (24)	86 (14)

[a] Asterisk indicates equivalent isotropic U defined as one-third of the trace of the orthogonalized U_{ij} tensor.

Table IV. Anisotropic Thermal Parameters ($Å^2 \times 10^3$)[a]

	U_{11}	U_{22}	U_{33}	U_{23}	U_{13}	U_{12}
Cu(1)	35 (3)	42 (3)	45 (3)	-2 (3)	8 (2)	-12 (2)
Cu(2)	38 (3)	44 (3)	32 (3)	-1 (2)	9 (2)	-10 (2)
Cu(3)	40 (3)	44 (3)	26 (3)	-4 (2)	13 (2)	-14 (2)
Cu(4)	29 (3)	40 (3)	39 (3)	-3 (2)	5 (2)	-3 (2)
Br(1)	39 (2)	38 (2)	37 (2)	-6 (2)	6 (2)	-10 (2)
Br(2)	58 (3)	62 (3)	28 (2)	-5 (2)	18 (2)	-13 (2)
Br(3)	35 (2)	43 (2)	25 (2)	3 (2)	4 (2)	-8 (2)
Br(4)	39 (2)	41 (3)	35 (2)	-3 (2)	14 (2)	-5 (2)
Br(5)	35 (2)	39 (2)	32 (2)	-2 (2)	9 (2)	-8 (2)
Br(6)	37 (2)	41 (3)	39 (2)	-8 (2)	4 (2)	-10 (2)
Br(7)	34 (2)	48 (3)	43 (3)	-3 (2)	13 (2)	-13 (2)
Br(8)	46 (2)	60 (3)	38 (2)	-13 (2)	14 (2)	-15 (2)
Br(9)	48 (3)	53 (3)	49 (3)	7 (2)	12 (2)	-8 (2)
Br(10)	72 (3)	47 (3)	62 (3)	-3 (2)	5 (2)	-24 (2)

[a] The anisotropic temperature factor exponent takes the form $-2\pi^2(h^2a^2U_{11} + ... + 2hka^*b^*U_{12})$.

Table V. Bond Lengths (Å)

Cu(1)-Br(1)	2.395 (5)	Cu(1)-Br(2)	2.369 (6)
Cu(1)-Br(3)	2.507 (6)	Cu(1)-Br(4)	2.471 (6)
Cu(2)-Br(3)	2.426 (5)	Cu(2)-Br(4)	2.390 (6)
Cu(2)-Br(5)	2.403 (6)	Cu(2)-Br(6)	2.400 (5)
Cu(3)-Br(5)	2.437 (5)	Cu(3)-Br(6)	2.436 (6)
Cu(3)-Br(7)	2.416 (6)	Cu(3)-Br(8)	2.407 (6)
Cu(4)-Br(7)	2.479 (5)	Cu(4)-Br(8)	2.433 (6)
Cu(4)-Br(9)	2.378 (6)	Cu(4)-Br(10)	2.370 (6)
N(1)-C(11)	1.525 (50)	N(1)-C(12)	1.502 (56)
N(1)-C(13)	1.495 (53)	N(2)-C(21)	1.534 (57)
N(2)-C(22)	1.455 (48)	N(2)-C(23)	1.449 (50)

in Tables V, VI, and VII. A table listing observed and calculated structure factors has been deposited as supplementary material.

Structure Description. The crystal structure of $TMA_2Cu_4Br_{10}$ [TMA = $(CH_3)_3NH^+$] is built up of nearly planar, bibridged $Cu_4Br_{10}^{2-}$ units which aggregate to form infinite stacks parallel to the crystallographic a axis. The trimethylammonium ions hydrogen bond to the tetramers, terminating the oligomers at $n = 4$. The structure is similar, but not identical with, the corresponding chloride salt.

Within the tetrameric species, each copper ion has a near square-planar coordination geometry, as seen in Figure 7. The Cu–Br distances within the tetramer range from 2.369 to 2.507 Å. As expected, the terminal Cu–Br distances are short (<2.4 Å) but the interior distances show a surprising variation, ranging from 2.390 to 2.507 Å. The interior Br–Cu–Br angles are generally less than 90°, as is normal in these bibridged systems. The bridging Cu–Br–Cu angles, of importance magnetically, show an interesting variation, with the outer angles averaging 94.8° while the central angles (at Br(5) and Br(6)) average 92.2°. This difference is significant magnetically and should be recognizable in the compound's magnetic behavior. The smaller central angles are a direct reflection of the abnormally short Cu–Br distances to Br(5) and Br(6).

Table VI. Bond Angles (deg)

Br(1)-Cu(1)-Br(2)	95.6 (2)	Br(1)-Cu(1)-Br(3)	89.4 (2)
Br(2)-Cu(1)-Br(3)	171.5 (2)	Br(1)-Cu(1)-Br(4)	168.0 (2)
Br(2)-Cu(1)-Br(4)	90.6 (2)	Br(3)-Cu(1)-Br(4)	83.4 (2)
Br(3)-Cu(2)-Br(4)	86.8 (2)	Br(3)-Cu(2)-Br(5)	92.4 (2)
Br(4)-Cu(2)-Br(5)	176.1 (2)	Br(3)-Cu(2)-Br(6)	179.2 (3)
Br(4)-Cu(2)-Br(6)	92.5 (2)	Br(5)-Cu(2)-Br(6)	88.3 (2)
Br(5)-Cu(3)-Br(6)	86.7 (2)	Br(5)-Cu(3)-Br(7)	93.0 (2)
Br(6)-Cu(3)-Br(7)	169.8 (2)	Br(5)-Cu(3)-Br(8)	171.7 (2)
Br(6)-Cu(3)-Br(8)	92.8 (2)	Br(7)-Cu(3)-Br(8)	86.0 (2)
Br(7)-Cu(4)-Br(8)	84.1 (2)	Br(7)-Cu(4)-Br(9)	90.5 (2)
Br(8)-Cu(4)-Br(9)	174.5 (2)	Br(7)-Cu(4)-Br(10)	166.0 (2)
Br(8)-Cu(4)-Br(10)	90.6 (2)	Br(9)-Cu(4)-Br(10)	94.4 (2)
Cu(1)-Br(3)-Cu(2)	93.8 (2)	Cu(1)-Br(4)-Cu(2)	95.7 (2)
Cu(2)-Br(5)-Cu(3)	92.2 (2)	Cu(2)-Br(6)-Cu(3)	92.3 (2)
Cu(3)-Br(7)-Cu(4)	94.2 (2)	Cu(3)-Br(8)-Cu(4)	95.6 (2)
C(11)-N(1)-C(12)	115.2 (32)	C(11)-N(1)-C(13)	109.8 (28)
C(12)-N(1)-C(13)	110.3 (28)	C(21)-N(2)-C(22)	114.1 (29)
C(21)-N(2)-C(23)	109.0 (30)	C(22)-N(2)-C(23)	116.3 (31)

Table VII. Interatetramer Distance and Angles

distances, Å		angles, deg	
Cu(1)-Br(9)[a]	2.981 (6)	Cu(1)-Br(9)[a]-Cu(4)[a]	100.1 (2)
Cu(2)-Br(7)[a]	3.193 (6)	Cu(2)-Br(7)[a]-Cu(3)[a]	93.6 (2)
		Cu(2)-Br(7)[a]-Cu(4)[a]	89.2 (2)
Cu(3)-Br(5)[a]	3.392 (6)	Cu(3)-Br(5)[a]-Cu(2)[a]	89.1 (2)
		Cu(3)-Br(5)[a]-Cu(3)[a]	96.3 (2)
Cu(4)-Br(3)[a]	3.113 (6)	Cu(4)-Br(3)[a]-Cu(1)[a]	88.3 (2)
		Cu(4)-Br(3)[a]-Cu(2)[a]	92.6 (2)
Cu(1)-Br(5)[b]	3.353 (6)	Cu(1)-Br(5)[b]-Cu(2)[b]	92.5 (2)
		Cu(1)-Br(5)[b]-Cu(3)[b]	86.7 (2)
Cu(2)-Br(3)[b]	3.341 (6)	Cu(2)-Br(3)[b]-Cu(1)[b]	90.9 (2)
		Cu(2)-Br(3)[b]-Cu(2)[b]	93.6 (2)
Cu(3)-Br(1)[b]	2.876 (6)	Cu(3)-Br(1)[b]-Cu(1)[b]	99.2 (2)

[a] $1 - x, 1 - y, 1 - z$. [b] $-x, 1 - y, 1 - z$.

Table VIII. Least-Squares Plane for the $Cu_4Br_{10}^{2-}$ Tetramer

$-0.6576x + 0.6502y - 0.3466z - 1.1031 = 0$

atom	distance, Å	atom	distance, Å
Cu(1)	-0.121 (4)	Br(5)	-0.004 (3)
Cu(2)	-0.096 (4)	Br(6)	-0.164 (3)
Cu(3)	0.158 (4)	Br(7)	0.051 (4)
Cu(4)	-0.116 (4)	Br(8)	-0.027 (4)
Br(1)	0.198 (3)	Br(9)	-0.136 (4)
Br(2)	0.033 (4)	Br(10)	0.268 (4)
Br(3)	-0.015 (3)	N(1)	2.48 (3)
Br(4)	-0.028 (3)	N(2)	-0.86 (3)

The tetramer shows significant deviations from planarity (Table VIII). The hydrogen bonding between N(2) and Br(10) appears to push that latter atom significantly out of the plane (0.268 Å) and leads to the large deviation of the Br(7)–Cu(4)–Br(10) angle from 180°. At the other end of the tetramer, Br(1) tips toward Cu(3) on the adjacent tetramer, causing both of them to move significantly out of the least-squares plane (0.198 and 0.158 Å, respectively). This leads to a very short intertetramer interaction Cu(3)–Br(1)[b] of 2.88 Å. We see a general trend that the intertetramer distances are longer in the middle and shorter toward the ends.

The packing of the tetramers into stacks, as indicated in the previous section, leads to further semicoordination of the copper ions, giving a 4 + 2 coordination to three of the copper ions (Cu(1), Cu(2), and Cu(3)) and a 4 + 1 coordination for the fourth (Cu(4)). As seen in Table VII, interoligomer contacts range from 2.9 to 3.4 Å. Interestingly, although the stacking pattern alter-

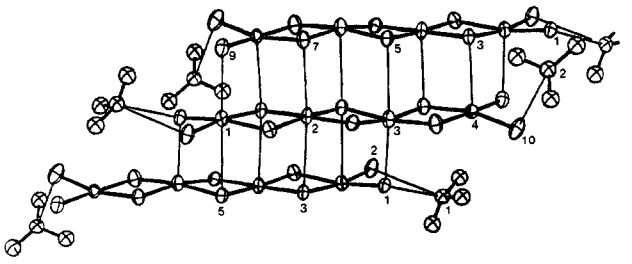

Figure 8. Illustration of the hydrogen bonding of the $(CH_3)_3NH^+$ ions to the $Cu_4Br_{10}^{2-}$ tetramers.

nates, the distances between the least-squares planes are virtually identical with 3.233 Å for the $(^1/_2,-^1/_2)$ stack and 3.228 Å for the $(^3/_2,^1/_2)$ stack.

The unusual stacking pattern assumed by the tetramers is related to the hydrogen bonding of the trimethylammonium ions. N(1) forms a bifurcated hydrogen bond to Br(1) and Br(2), while N(2) forms a single hydrogen bond to Br(10) (Figure 8). In contrast, for the uniform stacks in $(TMA)_2Cu_4Cl_{10}$, the crystallographic equivalent TMA ions both form bifurcated hydrogen bonds. In the bromide, the packing associated with the second TMA ion apparently allows the stacking to assume its unusual arrangement. This difference may be related to the larger ionic radius of the bromide ions, allowing more (or less) room for the TMA ion to orient itself in a favorable manner.

The magnetic properties of $[TMA]_2Cu_4Br_{10}$ have been examined by using a vibrating sample magnetometer. The magnetic susceptibility χ of a powder sample is less than 0.001 emu/mol from 50 to 300 K with a slight maximum around 200 K. The very low value of χ is consistent with a singlet ground state of the tetramer. We interpret the maximum in the susceptibility as a Bleaney–Bowers-like susceptibility, with the system collapsing into the singlet ground state at temperatures below about 200 K. Therefore, no long-range ordering is assumed to take place. Due to the small value of the susceptibility no additional details are available at this time. We can conclude, however, that the compound is strongly coupled in an antiferromagnetic sense with exchange constants, J/k, of several hundred degrees. This is consistent with the structural properties of this compound.[2,12,19] Further details with be published later.[35]

Finally, it is interesting to note the difference in crystal chemistry between the $(CH_3)_3NHCl$–$CuCl_2$ and the $(CH_3)_3NHBr$–$CuBr_2$ systems. In addition to the subtle differences between the tetrameric species, there are rather substantial differences when the other known compounds are compared. The chloride system exhibits a wealth of known compounds, including A_2CuCl_4,[35] $A_3Cu_2Cl_7$,[36,37] $ACuCl_3{\cdot}2H_2O$,[36,38] and $A_2Cu_4Cl_{10}$[34] [A = $(CH_3)_3NH^+$]. In addition, we have isolated two other salts:[39] a metastable, hexagonal $ACuCl_3$ compound and a compound crystallizing as flat plates with an apparent stoichiometry of $A_3Cu_4Cl_{11}$. The bromide system, the earlier report[9] not withstanding, appears to contain only two variants: the $A_2Cu_4Br_{10}$ salt reported here, and an A_2CuBr_4 salt isolated from solutions containing excess trimethylammonium bromide. It thus may be worthwhile pursuing further investigation to search for the analogous bromide salts and to further characterize this complex structural system.

Conclusion. The variable coordination behavior of the copper(II) ion, especially noticeable in its halide salts, leads to a wide variation in structural behavior. In particular, in the planar, bibridged oligomers, the intraoligomer square-planar coordination geometry, coupled with the option of formation of one or two semicordinate bonds to adjacent oligomers (or other ligands), yields a plethora of stacking patterns. The simple graphic representation, as well as the vector notation introduced, helps catalog and systematize the known patterns and also indicates what additional types might be expected to be observed in the future, as further compounds are studied.

The categorization of structural characteristics, however, fails to focus on the problem of why one pattern is preferred over another, or, more fundamentally, why one oligomer is formed rather than another of a different length (or even, why these types of oligomers are formed rather than polymeric species with other structural properties.[8]) Clearly, a delicate balance of crystal-field, ligand–ligand repulsion, hydrogen bonding strength, and other packing forces is involved which defies quantization at this time. It does provide a challenge, however, for the theorist interested in the prediction of crystal structures in complex systems.

Acknowledgment. This work was supported in part by NSF Grant DMR-8219430. The availability of magnetic data from Prof. J. E. Drumheller, prior to publication, is appreciated.

Note Added in Proof. We have recently determined the structures of several additional compounds containing various types of oligomers. These include the following (compound, pattern type): (tetramethylethylenediammonium)Cu_2X_6 (X = Cl^-, Br^-), $2(^3/_2,^1/_2)$; (3-methyl-2-aminopyridinium)$_2Cu_3Cl_8$, $3(^1/_2,^1/_2)$ $(^1/_2,-^1/_2)$; (*N*-methylphenethylammonium)$Cu_3Cl_7(C_2H_5OH)$, $3(^1/_2,^1/_2)$; (5-bromo-6-methyl-2-aminopyridnium)$_2Cu_3Cl_8$, $3(^1/_2,^1/_2)$; (5-methyl-2-aminopyridinium)$_2Cu_3Cl_8$, $3(^1/_2,^1/_2)$; $[(CH_3)_4N]_2Cu_4Cl_{10}$, $4(^3/_2,^1/_2)$; (4-methyl-2-aminopyridinium)$_2Cu_4Cl_{10}$, $4(^1/_2,^1/_2)$.

Also recently published in the literature is the structure of (benzimidazolium)$_2Cu_2Cl_6$, which has a $2(^1/_2,^1/_2)$ stacking pattern.[40]

The salts (dibenzotetrathiofulvalenium)$_2Cu_2X_6$ (X = Cl,Br) contain the first reports of isolated, planar $Cu_2X_6^{2-}$ ions.[41]

Registry No. $[(CH_3)_3NH]_2Cu_4Br_{10}$, 99398-67-1; Cu, 7440-50-8.

Supplementary Material Available: Tables of observed and calculated structure factors (8 pages). Ordering information is given on any current masthead page.

(35) Rubenacker, G. V.; Drumheller, J.; Emerson, K.; Geiser, U.; Willett, R. D. *J. Appl. Phys.*, in press.
(36) Remy, H.; Laves, G. *Ber. Dtsch. Chem. Ges. A* **1933**, *66*, 401.
(37) Clay, R. M.; Murray-Rust, P.; Murray-Rust, J. *J. Chem. Soc., Dalton Trans.* **1973**, 595.
(38) Losee, D. B.; McElearney, J. N.; Siegel, A.; Carlin, R. L.; Kahn, A. A.; Roux, J. P.; James, W. J. *Phys. Rev.* **1972**, *B6*, 4342.
(39) Willett, R. D., unpublished work.
(40) Bukowska-Strzyzewska, M.; Tosik, A.; Glowiak, T.; Wnek, J. *Acta Crystallogr.* **1985**, *C41*, 1184.
(41) Honda, M.; Katayama, C.; Tanaka, J.; Tanaka, M. *Acta Crystallogr. C*41 **1985**, 197, 688.